



Queensland University of Technology
Brisbane Australia

This is the author's version of a work that was submitted/accepted for publication in the following source:

Chang, Sunwoo, Clement, Prabhakar, [Simpson, Matthew](#), & Lee, Kang-Kun (2011) Does sea-level rise have an impact on saltwater intrusion? *Advances in Water Resources*, 34(10), pp. 1283-1291.

This file was downloaded from: <http://eprints.qut.edu.au/42002/>

© Copyright 2011 Elsevier

This is the author's version of a work that was accepted for publication in <Advances in Water Resources>. Changes resulting from the publishing process, such as peer review, editing, corrections, structural formatting, and other quality control mechanisms may not be reflected in this document. Changes may have been made to this work since it was submitted for publication. A definitive version was subsequently published in *Advances in Water Resources*, [VOL 34, ISSUE 10, (2011)] DOI: 10.1016/j.advwatres.2011.06.006

Notice: *Changes introduced as a result of publishing processes such as copy-editing and formatting may not be reflected in this document. For a definitive version of this work, please refer to the published source:*

<http://dx.doi.org/10.1016/j.advwatres.2011.06.006>

Does Sea-level Rise Have an Impact on Saltwater Intrusion?

Sun Woo Chang¹, T. Prabhakar Clement^{1*}, Matthew J. Simpson², Kang-Kun Lee³.

¹Department of Civil Engineering, 212 Harbert Engineering Center, Auburn University, Auburn, AL, USA 36849-5337

²Discipline of Mathematical Sciences, Queensland University of Technology, G.P.O. Box 2434, Brisbane, Queensland 4001, Australia

³School of Earth and Environmental Science, Seoul National University, Seoul 151-742, Korea

*Corresponding author

Phone : (+1) 334-844-6268

Fax: (+1) 334 -844-6290

Email : clemept@auburn.edu (Prabhakar Clement)

1 **Abstract**

2

3 Climate change effects are expected to substantially raise the average sea level. It is widely
4 assumed that this raise will have a severe adverse impact on saltwater intrusion processes in
5 coastal aquifers. In this study we hypothesize that a natural mechanism, identified as the “lifting
6 process” has the potential to mitigate or in some cases completely reverse the adverse intrusion
7 effects induced by sea-level rise. A detailed numerical study using the MODFLOW-family
8 computer code SEAWAT, was completed to test this hypothesis and to understand the effects of
9 this lifting process in both confined and unconfined systems. Our conceptual simulation results
10 show that if the ambient recharge remains constant, the sea-level rise will have no long-term
11 impact (i.e., it will not affect the steady-state salt wedge) on confined aquifers. Our transient
12 confined-flow simulations show a self-reversal mechanism where the wedge which will initially
13 intrude into the formation due to the sea-level rise would be naturally driven back to the original
14 position. In unconfined systems, the lifting process would have a lesser influence due to changes
15 in the value of effective transmissivity. A detailed sensitivity analysis was also completed to
16 understand the sensitivity of this self-reversal effect to various aquifer parameters.

17

18

19

20

21 **Keywords:** saltwater intrusion, sea-level rise, coastal aquifer, climate change, confined aquifer,
22 unconfined aquifer

1 **1. Introduction**

2 Saltwater intrusion is a serious environmental issue since eighty percent of the world's
3 population live along the coast and utilize local aquifers for their water supply. In the US alone,
4 it is estimated that freshwater aquifers along the Atlantic coast supply drinking water to 30
5 million residents living in coastal towns located from Maine to Florida [1]. Under natural
6 conditions, these coastal aquifers are recharged by rainfall events, and the recharged water
7 flowing towards the ocean would prevent saltwater from encroaching into the freshwater region.
8 However, over exploitation of coastal aquifers has resulted in reducing groundwater levels
9 (hence reduced natural flow) and this has led to severe saltwater intrusion. Cases of saltwater
10 intrusion, with varying degrees of severity and complexity, have been documented throughout
11 the Atlantic coastal zone. For example, in May County, New Jersey, more than 120 water supply
12 wells have been abandoned because of saltwater contamination [2]. A recent USGS [1] study
13 provides a summary of saltwater intrusion problems and various mitigation techniques.
14 International organizations have identified saltwater intrusion as one of the major environmental
15 issues faced by several coastal cities in India, China, and Mexico [3]. Researchers have also
16 reported that variations in the sea level and the associated wedge movement can influence the
17 near-shore and/or large-scale submarine discharge patterns and impact nutrient loading levels
18 across the aquifer-ocean interface [4-8]. Therefore, understanding the dynamics of saltwater
19 intrusion in coastal aquifers and its interconnection to anthropogenic activities is an important
20 environmental challenge.

21 While anthropogenic activities, such as over pumping and excess paving in urbanized
22 areas, are the major causes of saltwater intrusion, it is anticipated that increases in the sea level

1 due to climate change would aggravate the problem. Nevertheless, only a few studies have
2 focused on understanding the combined effects of climate change and anthropogenic impacts [4].
3 Feseker [9] completed a numerical modeling study to assess the impacts of climate change and
4 changes in land use patterns on the salt distribution in a coastal aquifer. The model used
5 parameters to reflect the conditions similar to those observed at the CAT-field site located in the
6 northern coast of Germany. The study concluded that rising sea level could induce rapid
7 progression of saltwater intrusion. Furthermore, the time scale of changes resulting from the
8 altered boundary conditions could take decades or even centuries to impact groundwater flows
9 and hence the present day salt distribution might not reflect the long term equilibrium conditions.
10 Leatherman [10] investigated the effects of rising sea-level on salinization in an aquifer in Texas.
11 Meisler et al.[11] used a finite-difference computer model to analyze the effect of sea-level
12 changes on the development of the transition zone between fresh groundwater and saltwater in
13 the northern Atlantic Coastal Plain (from New Jersey to North Carolina). Navoy [12] studied
14 aquifer-estuary interactions to assess the vulnerability of groundwater supplies to sea level rise-
15 driven saltwater intrusion in a coastal aquifer in New Jersey. Essink [13] used a three-
16 dimensional transient density-driven groundwater flow model to simulate saltwater intrusion in a
17 coastal aquifer in the Netherlands for three types of sea-level rise scenarios: no rise, a sea-level
18 rise of 0.5 m per century, and a sea-level fall of 0.5 m per century. They concluded that sea level
19 rise of 0.5 m per century would increase the salinity in all low-lying regions closer to the sea.
20 Dausman and Langevin [14] completed SEAWAT simulations for a coastal aquifer in Broward
21 County, Florida, and demonstrated that if the sea-level rise becomes greater than 48 cm over the
22 next 100 years then several local well fields would be vulnerable to chloride contamination.
23 Melloul and Collin [15] evaluated the potential of sea-level rise to cause permanent freshwater

1 reserve losses in a coastal aquifer in Israel. They quantified the saltwater intrusion effect due the
2 lateral movement of seawater and due changes in the groundwater head. For the assumed sea-
3 level rise of 0.5 m, about 77% of the loss was due to the lateral movement and about 23% was
4 due to the head change. Ranjan et al. [16] used the sharp interface assumption to analyze the
5 effects of climate change and land use on coastal groundwater resources in Sri Lanka.
6 Giambastiani et al. [17] conducted a numerical study to investigate saltwater intrusion in an
7 unconfined coastal aquifer of Ravenna, Italy. Their result showed that the mixing zone between
8 fresh and saline groundwater will be shifted by about 800 m farther inland for a 0.475 m per
9 century of sea-level rise. Loaiciga et al. [18] employed hydrogeological data and the finite-
10 element numerical model FEFLOW to assess the likely impacts of sea-level riser and
11 groundwater extraction on seawater intrusion in the Seaside Area aquifer of Monterrey County,
12 California, USA. Sea-level rise scenarios were consistent with current estimates made for the
13 California coast, and varied between 0.5 and 1.0 m over the 21st century. These authors
14 concluded that sea-level rise would have a minor contribution to seawater intrusion in the study
15 area compared to the contribution expected from groundwater extraction.

16 The primary focus of most of the field-scale modeling studies discussed above was to understand
17 saltwater intrusion problems related to a specific field site. More recently, Werner and Simmons
18 [19] completed a conceptual modeling study using a steady-state, sharp-interface analytical
19 model and focused on developing a general understanding of the impacts of sea-level rise on
20 groundwater aquifers that might have different types of boundary conditions. They used a
21 relatively simple analytical model to provide a first-order assessment of the impacts of sea level
22 changes on saltwater intrusion on aquifer systems with two types of boundary conditions. Their
23 results showed that the level of intrusion would depend on the type of inland boundary condition

1 assumed in the model. The steady-state, sharp-interface, analytical expression used in the study
2 did not consider saltwater mixing effects and transient effects. The transient effects in
3 unconfined aquifers were later investigated by Webb and Howard [20], using a numerical model
4 that employed constant head boundary conditions, to study the changes in the rates of intrusion
5 for a range of hydro-geological parameters.

6 The objective of this study is to complete a comprehensive investigation of the transient
7 impacts of the sea-level rise on saltwater intrusion processes in both confined and unconfined
8 coastal aquifer systems that are driven by natural recharge fluxes. The results are then used to
9 develop an intuitive understanding for saltwater intrusion dynamics, which can help better asses
10 and manage the potential long term impacts of sea-level rise on coastal aquifers.

11

12 **2. Problem Formulation and Conceptual Modeling**

13 A general conceptual model for describing a groundwater flow system near a coastal boundary is
14 shown in Figure 1a. As shown in the figure, under natural flow conditions, the dense sea water
15 would have the tendency to intrude beneath the fresh groundwater. The spatial extent of the
16 intruded saltwater wedge (designated as the “toe position X_T ”) would depend on several aquifer
17 parameters including recharge rate, regional aquifer discharge rate, hydraulic properties, and the
18 sea level. Recent climate change studies have shown that the global sea-level, on average, is
19 expected to rise between 18 and 59 cm this century [21]. Worst-case projections show it could
20 be as high as 180 cm [22]. Therefore, environmental planners worldwide are seriously
21 concerned about the impacts of sea-level rise on saltwater intrusion processes, especially in over-

1 utilized, urbanized coastal aquifers that already have low groundwater levels. Currently, it is
2 expected that the rising sea level will enhance saltwater intrusion and potentially contaminate
3 many freshwater reserves. Figure 1b depicts a commonly assumed conceptual model [19, 23-27]
4 that illustrates how the rising sea level would impact the groundwater quality by forcing the
5 wedge to migrate inland. This conceptual model, however, ignores the fact that when the
6 seawater rises at the sea-side boundary the system would pressurize and the water-table level
7 might be “lifted” throughout the aquifer. Figure 1c illustrates a revised conceptual model. This
8 revised model accounts for the lift in the groundwater level over the entire system due to the
9 changes in the sea-side boundary condition. It is expected that after a long period (i.e., at or near
10 steady state) this lifting effect would approximately raise the entire fresh water body (measured
11 from the bottom of the aquifer) by an extent similar to the sea-level rise (i.e., a similar order of
12 magnitude). One could intuitively expect this lifting mechanism to counteract and reduce the
13 impacts due to the sea-level rise. However, it is unclear to what extent this lifting process could
14 reduce the overall impacts due to sea-level rise. In this study, we employ this revised conceptual
15 model to hypothesize that changes in the sea-level might have little or no impact on saltwater
16 intrusion when the net flux through the system is unchanged. The overall goal of this conceptual
17 study is to test the validity of this hypothesis, and understand its ramifications under transient
18 conditions in idealistic confined and unconfined systems.

19

20 **3. Details of the Numerical Experiment**

21 The base-case problem considered in this study was adapted from Werner and Simmons’
22 conceptual model [19] of a seawater intrusion field study completed in Pioneer Valley, Australia.

1 The original problem only considered unconfined flow conditions; in this work, the problem was
2 modified to investigate both confined and unconfined conditions. Our numerical study
3 considered a two-dimensional aquifer system which is 1000 m long and 30 m thick. A
4 rectangular numerical grid, with $\Delta x = 4$ m, $\Delta y = 1$ m and $\Delta z = 0.4$ m, was used. The initial sea
5 level (prior to the rise) was assumed to be at 30 m and the sea level was then allowed to rise
6 instantaneously to 34 m. The net sea-level rise assumed was 4 m, a theoretical worst-case
7 scenario which is approximately double the extreme value predicted by Vermeer and Rahmstorf
8 [22]. The assumed sea-level rise was chosen to approximately mimic the last interglacial
9 period's rapid sea-level rise that reached up to 4 to 6 m due to rapid loss of ice-sheet [28]. It is
10 important to note that this is not a "true" scenario simulation exercise; our objective is not to
11 forecast the future location of saltwater wedge for a specific system, rather it is to develop a
12 generic conceptual understanding to assess the potential impacts of sea-level rise on saltwater
13 intrusion processes. Therefore, some extreme sea-level rise scenarios were initially simulated (as
14 the base-case) to better illustrate certain subtle transport mechanisms. Later, as a part of the
15 sensitivity analysis, we explore some realistic sea-level rise scenarios that range from 0.2 m
16 (minimum rise predicted by IPCC) to 4 m (double the maximum rise predicted by Vermeer and
17 Rahmstorf [22]). Also, in all base-case simulations we assumed instantaneous rise (a worst-case
18 scenario) and later in the sensitivity section we have presented the results for other finite rates of
19 sea-level rise.

20 The seawater density was assumed to be $1,025 \text{ kg/m}^3$ with salt concentration of 35 kg/m^3 .
21 The regional groundwater flux supplied through the right boundary using a set of artificial
22 injection well nodes. The flux (q , flow per unit depth) supplied from the right boundary was
23 $0.005 \text{ m}^2/\text{day}$ (or a total flow rate (Q) of $0.15 \text{ m}^3/\text{day}$ over the 30 m thick aquifer). Recharge (W)

1 flow was delivered from the top boundary at the rate of 5×10^{-5} m/day. These regional and
2 recharge flows were simply selected to locate the initial location of the saltwater toe in between
3 300 to 500 m. The hydraulic conductivity was set to 10 m/day, specific storage was set to 0.008
4 m^{-1} in each confined layer, and porosity to 0.35. Longitudinal and transversal dispersivity values
5 were assigned to be 1 m and 0.1 m, respectively. The initial sea level was set at 30 m to simulate
6 a base-case steady-state wedge. This steady-state wedge was later used as the initial condition in
7 all subsequent sea-level rise simulations.

8 The MODFLOW-family variable density flow code SEAWAT [29] was used in this
9 study with the central difference weighting option. The modeling approach was validated by
10 solving Henry's steady-state solution [30] [31] and also laboratory data provided by Goswami
11 and Clement [32], and Abarca and Clement [33]. Several sets of numerical experiments were
12 completed to explore various types of flow conditions and parameter values. The first set of
13 experiments only considered confined-flow conditions and the results were used to explore
14 certain novel salt-wedge reversal mechanisms that have not been reported in the published
15 literature. Later simulations consider both confined and unconfined flow conditions.

16 **4. Results and Discussions**

17 **4.1. Impacts of sea-level rise on confined flow conditions**

18 The goal of the first steady-state simulation is to estimate the initial saltwater wedge profile that
19 would exist in the system prior to sea-level rise. Figure 2 (continuous line) shows the 50%
20 isochlor of the initial steady-state concentration profile for the base-case, confined-flow system.
21 This 50% concentration profile is defined as the base saltwater wedge. The figure shows that
22 under the assumed groundwater flow conditions, the toe of the salt wedge advanced to 382 m

1 into the aquifer before sea-level rise. This steady-state condition was used as the initial condition
2 in all subsequent simulations.

3 The second steady-state simulation aimed to predict the long-term salt-wedge profile
4 after the sea-level rise. The water level at the seaside boundary was abruptly increased from 30
5 to 34 m to simulate an instantaneous sea-level rise. The system was allowed to evolve for
6 80,000 days to reach steady-state conditions. The new steady-state solution for the salt wedge
7 simulated by the model after raising the sea level is also shown in Figure 2 (using circle data
8 points). Interestingly, and rather surprisingly, the model-predicted saltwater profiles for both
9 conditions (pre and post sea-level rise) were identical, indicating that the sea-level rise will have
10 absolutely no impact on the location of the steady-state wedge when the freshwater flux
11 transmitted through the system remained constant (i.e., if the rainfall/recharge pattern was not
12 changed). This non-intuitive result has several important practical implications. The result
13 indicates that the lifting effect postulated in the conceptual model described in Figure 1c will
14 fully offset the negative impacts of sea-level rise in constant flux confined flow systems.

15 To further explore this result, we present the transient evolution of the location of the
16 saltwater wedge in Figure 3. These profiles show that when the sea-level was instantaneously
17 raised, the wedge initially started to move inward; however, after about 8,000 days, the direction
18 of wedge movement reversed and the wedge started to move backward until it reached the initial
19 steady-state profile. As far as we are aware, no one has predicted or postulated this self-reversal
20 mechanism. Understanding this self-reversal process has an enormous implication on how water
21 resources managers would perceive and manage the impacts of sea-level rise on saltwater
22 intrusion.

1 Figure 4 shows the transient variations in the toe position of the saltwater wedge (X_T).
2 The data shows that, under assumed flow conditions, the salt wedge first advanced into the
3 aquifer for about 8,000 days and reached a maximum distance of 432 m (from the sea boundary)
4 and then started to recede. The figure also shows the simulated transient freshwater head levels
5 at the right side boundary. This freshwater head data is an excellent surrogate for quantifying the
6 progression of the aquifer “lifting” process, postulated in Figure 1c. This dataset shows that the
7 initial head at the right boundary, as predicted by the model prior to the sea-level rise, was 31 m.
8 When the sea-level was raised instantaneously from 30 to 34 m, it took about 2,000 days for the
9 right boundary to fully respond to this change. After about 2,000 days, the fresh-water level in
10 the right boundary reached a constant value of about 35 m. The net change in the freshwater
11 level was about 4 m, almost identical to the sea-level rise forced at the left boundary. This
12 implies that the raising seaward-boundary head lifted the entire fresh groundwater system by a
13 similar order of magnitude. This lifting process was able to fully reverse the salt wedge location.
14 The rate of the reversal process would depend on rate at which the groundwater system was
15 lifted (or how quickly the groundwater heads would respond), which would in turn depend on the
16 storage properties of the aquifer and the rate of sea-level rise. In the following section, we
17 provide a detailed analysis that quantifies the sensitivity of the self-reversal process to the value
18 of storage coefficient, rate of sea-level rise and the magnitude of rise. All these simulations used
19 the base-case steady-state solution as the initial condition.

20

21 **4.2. Sensitivity analysis of the self-reversal process in confined systems**

22 4.2.1. Sensitivity to specific storage

1 We first explored the sensitivity of the intrusion mechanism to various values of specific storage
2 (S_s). In this analysis, the value of S_s was varied by an order magnitude with the range 0.0008 to
3 0.008 m^{-1} . In all sensitivity simulations, the other parameters were fixed at base-case levels
4 shown in Table 1. Figure 5a shows the temporal variations in the toe position (X_T) for different
5 values of S_s . The data shows that when S_s was small the system responded rapidly and the
6 intrusion effect was reversed quickly. Also, the maximum intrusion length was small for smaller
7 values of S_s . The maximum values of the predicted saltwater toe position (X_T) were 432, 412,
8 394, and 386 m for the S_s values 0.008, 0.005, 0.002 and 0.0008 m^{-1} , respectively. The figure
9 shows that when S_s is small (at 0.0008 m^{-1}) the change in the salt wedge location was relatively
10 small even for an extreme sea-level rise of 4 m. The total time required to reach the maximum
11 intrusion level (defined as the duration of intrusion) was 6,000 to 8,000 days. These values
12 appear to be relatively insensitive to S_s . Overall, the extent of saltwater intrusion as indicated by
13 the maximum value of X_T was more sensitive to S_s than the duration of intrusion.

14 4.2.2. Sensitivity to the magnitude of sea-level rise

15 The sensitivity of the intrusion length to the magnitude of the sea-level rise was explored by
16 varying the sea level rise within the range of 0.2 to 4 m. Figure 5b shows the transient variations
17 in X_T values for various values of sea-level rise. The maximum values of X_T were
18 approximately proportional to the magnitude of sea-level rise. Also, similar to the previous
19 sensitivity experiment, the time taken to reach the maximum values was about 6,000 to 8,000
20 days, and this time was relatively insensitive to the magnitude of the sea-level rise.

21 4.2.3. Sensitivity to the rate of sea-level rise

1 Simulations were completed to test the sensitivity of the intrusion process to changes in the rate
2 of sea-level rise. Literature data indicated that the current rate of sea-level rise, observed
3 worldwide, has ranged from 2 to 4 mm/year [34]. Climate change model projections, however,
4 show that the global rate could at least double by the end of this century [35]. A total rise of 4 m
5 was simulated using six different rate scenarios: instantaneous, 1 mm/day for 4,000 days, 0.1
6 mm/day for 40,000 days, 0.05 mm/day for 80,000 days, and infinite rise at a rate of 0.04 mm/day
7 with $S_s = 0.008$ and $S_s = 0.0008$. Figure 5c shows the temporal variations in the simulated toe
8 position (X_T) for all five scenarios. The data demonstrates that the rate of the self-reversal
9 process would depend on the sea-level rise rate. When the rate of rise was low the reversal cycle
10 had a longer duration. The maximum value of the intrusion length, X_T , decreased with decrease
11 in the rate of sea-level intrusion. The time taken to reach the maximum level of intrusion was
12 7,500, 10,000, 40,000 and 80,000 days for instantaneous, 1 mm/day, 0.1 mm/day, 0.05 mm/day
13 sea-level rise rates, respectively. When sea-level was allowed to rise infinitely at a fixed rate, the
14 results reached an irreversible, quasi steady-state level. It is important to note this irreversible
15 intrusion level was primarily an artifact due the relatively large storage value (of 0.008 m^{-1})
16 assumed as the base-case parameter. When we reduced the specific storage value by an order of
17 magnitude (to 0.0008 m^{-1} , a more typical value for confined flow) the head information
18 propagated quickly and the lifting effect became continuously active. Therefore, the system with
19 a higher S_s value experienced immediate reversal and experienced very little intrusion under the
20 continuous-rise scenario. Overall, changes in the rate of sea-level rise influenced the maximum
21 level of intrusion as well as the time required to reach the maximum level. The time required to
22 reach the maximum would, to a large extent, depended on how long the sea rise occurred.

23

4.2.4. Sensitivity to dispersivity values

We explored the sensitivity of the intrusion mechanism to dispersivity coefficients by varying the value within the range of 0.5 m to 2 m for longitudinal dispersivity, α_L , and 0.05 m to 0.2 m for transverse dispersivity, α_T . As Abarca et al [36] pointed out, changing the values of dispersivity would impact the value of X_T (initial X_T decreased when the dispersivity coefficients were increased). Therefore, we defined a parameter “net change in salt wedge location,” which was computed as: maximum value of X_T - initial position of X_T , to quantify the changes. Figure 5d shows the temporal variations in the toe position (X_T) for different values of dispersivity. The net change in the salt wedge location was in between 44 and 53 m. The time taken to reach the maximum intrusion level and the peak of X_T values were relatively insensitive to changes in the value of dispersivity coefficient.

4.2.5. Sensitivity to other hydrological parameters

It is important to note that the transient reversal patterns would depend on the values of hydraulic conductivity, recharge rate and ambient groundwater flow. Sensitivity to variations in all these model parameters was also explored in this study. Simpler analytical solutions can be used to intuitively infer the sensitivity to individual variations in K , W and Q values under steady conditions. Werner and Simmons [19] followed this approach and completed a detailed sensitivity assessment for a steady-state unconfined problem. In this study, we present the results of selected number of sensitivity tests completed for a transient confined aquifer system using SEAWAT. Figure 6a shows the transient variations in X_T values for different hydraulic conductivity values; K values used are: 5 m/day, 10 m/day and 15 m/day. It should be noted that the simulated profiles have different initial X_T since individually changing any one of these

1 parameters (K, W or Q) would alter the steady-state solution of the base problem. The results
2 show that the peak value of X_T was increased and responding time was short (as expected) when
3 the K value was decreased. Figure 6b shows the transient variations in X_T values for various
4 values of Q and W (0.67×base values: Q = 0.1 m³/day and W = 3.3×10⁻⁵ m/day; base values: Q
5 = 0.15 m³/day and W = 5×10⁻⁵ m/day; doubled the base values: Q = 0.3 m³/day and W = 1×10⁻⁴
6 m/day). The data show that when the amount of freshwater flow was increased the peak value of
7 X_T increased and system also had a shorter responding time. It should be noted that if the
8 transport parameters were scaled consistently (for example, increase K and reduce the Q by a
9 similar factor) then there will be very little variation in the peak value of X_T .

10

11

12 **4.3. Impacts of sea-level rise on unconfined Aquifers**

13 To examine the impacts of sea-level rise on unconfined flow conditions, we completed
14 numerical simulations of an unconfined aquifer with dimensions identical to those used in the
15 confined simulation, except the top layer was modified to simulate unconfined flow. The length
16 of the unconfined aquifer was 1,000 m and the total thickness was 35 m. A numerical grid with
17 $\Delta x = 4$ m, $\Delta y = 1$ m and $\Delta z = 0.4$ m (75 confined layers), and a top unconfined layer of $\Delta z = 5$ m
18 was used. In all unconfined flow simulations, the value of average hydraulic conductivity was set
19 to 10 m/day, total regional freshwater flow (Q) from the right boundary was set to 0.15 m³/day,
20 and the areal recharge flux (W) was set to 5×10⁻⁵ m/day. In order to compare unconfined flow
21 simulation results against confined flow results, an identical instantaneous sea-level rise (rise

1 from 30 to 34 m) scenario was assumed. The specific storage, S_s , was set to 0.008 m^{-1} for all
2 confined layers, and specific yield, S_y , was set to 0.1 for the top unconfined layer.

3 We first completed a base-case, steady-state simulation for the unconfined system to generate
4 the initial conditions that existed prior to the sea level rise. Figure 7 compares the steady-state
5 salt wedge predicted for the unconfined flow system with the wedge predicted for a similar
6 confined flow system (data from Figure 2). The figure shows the both wedges are almost
7 identical, indicating that both confined and unconfined systems would behave in a similar
8 manner at steady-state conditions. The similarity between the two steady-state solutions can also
9 be explained mathematically, as shown in Appendix A.

10 To understand the impacts of sea-level rise on the unconfined aquifer, we instantaneously
11 raised the sea-level by 4 m and let the system reach steady state. Figure 8 compares the initial
12 and final steady-state saltwater wedge profiles in the unconfined system (dotted and continuous
13 lines). These profiles show that, unlike the confined system (compare with Figure 3 results), the
14 saltwater intrusion process is not reversible for the unconfined system. In unconfined aquifers,
15 the initial location of the toe XT_i and the final location of the toe position XT_f are distinctly
16 different. This is because, under unconfined conditions, the sea-level rise increases in the
17 saturated thickness (or transmissivity) of the aquifer. This increased transmissivity allows the
18 wedge to penetrate further into the system, resulting in a new steady-state condition. Comparing
19 the initial and final salt-wedge profiles indicates the initial salt wedge was approximately raised
20 by 4 m, similar to the level of sea-level rise. The groundwater level also rose over the entire
21 aquifer by about 4 m (as illustrated in Figure 1c), all the way to the inland boundary (the
22 predicted groundwater raise at the inland boundary was similar to the data shown in Figure 4).

1 These data indicate that the aquifer lifting process is active in the unconfined system. The lifting
2 process, however, was not able to fully reverse the wedge location since the system evolved from
3 a steady-state solution for the 30-m thick aquifer (with initial toe, XT_i , at about 382 m) to a new
4 steady-state solution for the 34-m thick aquifer (with final toe, XT_f , at about 510 m). The data
5 points (marked with circles) shown in the figure are steady-state wedge data predicted for a 34-m
6 thick “equivalent confined aquifer.” As expected (see Appendix A for an analytical analysis),
7 the final unconfined steady-state solution matched with an equivalent confined aquifer solution
8 with an appropriate value of aquifer thickness.

9 Figure 9 compares the results of transient changes in toe length predicted for the
10 following three systems: Case-1) standard base-case confined system of 30 m thickness (same as
11 the data shown in Figure 4); Case-2) unconfined flow system with base-case parameters; and
12 Case-3) unconfined system with very high S_s value (0.02 m^{-1}). It is important to note the S_s value
13 used for Case-3 is unrealistically high and this conceptual simulation was completed to
14 demonstrate the existence of certain subtle self-reversal mechanisms. Several observations can
15 be made from the results presented in Figure 9. All three solution started at the initial toe
16 location $XT_i = 382 \text{ m}$ and for about 1,000 days the unconfined solutions were approximately
17 equal to the confined flow solution. After this time, the unconfined model solutions started to
18 diverge. The Case-2 unconfined flow simulation reached the final steady-state toe position, XT_f ,
19 after about 50,000 days, and the system did not show any reversal effect. However, when we
20 repeated the unconfined simulation using high S_s values (Case-3) we could clearly observe the
21 reversal effect. Also, as expected, Case-3 required more time (about 100,000 days) to reach
22 steady-state final toe position XT_f . In summary, the aquifer lifting effect is active in unconfined
23 systems but it is difficult to observe any reversal effects in transient unconfined systems due to

1 the changes in the aquifer transmissivity. When an appropriate value of aquifer thickness was
2 used, the steady-solution for an unconfined flow system would be almost identical to an
3 “equivalent confined flow system.” The storage available within fully-saturated layers (which
4 act as confined layers) are typically very low and this would allow rapid propagation of head
5 perturbations; therefore, it is difficult to observe reversal effects in any realistic unconfined
6 aquifers.

7 **5. Conclusions**

8 Detailed numerical experiments were completed using the MODFLOW-family computer code
9 SEAWAT to study the transient effects of sea-level rise on saltwater wedge in confined and
10 unconfined aquifers with vertical sea-land interface. The simulation results show that if the
11 ambient recharge remains constant, the sea-level rise will have no impact on the steady-state salt
12 wedge in confined aquifers. The transient confined-flow simulations help identify an interesting
13 self-reversal mechanism where the wedge, which initially intrudes into the formation due to sea-
14 level rise, would be naturally driven back to the original position. However, in unconfined-flow
15 systems this self-reversal mechanism would have lesser effect due to changes in the value of the
16 effective transmissivity (or average aquifer thickness). Both confined and unconfined simulation
17 experiments show that rising seas would lift the entire aquifer and this lifting process would help
18 alleviate the overall long-term impacts of saltwater intrusion.

19 The sensitivity simulations show that the rate and the extent of the self-reversal process
20 would depend on the value of specific storage (S_s) and the rate of sea-level rise. When the rate
21 of rise was low the reversal cycle had a larger duration. Overall, the changes in the rate of sea
22 rise had relatively less influence on the maximum level of intrusion and more influence on the

1 and the time taken to reach the maximum level. On the other hand, variation in S_s values was
2 more sensitive to the maximum level of intrusion than the duration of intrusion (the time taken to
3 reach the maximum value).

4 It is important to note that the results presented in the conceptual modeling study are
5 based on simulations completed for idealized rectangular aquifers with homogeneous aquifer
6 properties. While the results are useful for developing a large-scale conceptual understanding of
7 the impacts of sea-level rise, evaluation of true impacts would require detailed site-specific
8 modeling efforts [18, 37]. A better understanding the self-reversal mechanism (both its spatial
9 and time scales), identified in this study, would have an enormous implication on managing the
10 impacts of sea-level rise in coastal groundwater aquifers. The results, however, do not imply that
11 one could simply ignore climate change effects on saltwater intrusion process. Rather it implies
12 that we can minimize its risks based on a sound scientific understanding of the transport
13 processes and by developing pro-active management strategies that are appropriate to unconfined
14 aquifers and confined aquifers. It is important to note that this study assumes the fluxes in the
15 system would remain constant. However, site-specific climate change effects could greatly alter
16 the recharge and regional fluxes (these natural hydrological fluxes can change due to variations
17 in the rainfall patterns), therefore the overall problem should be managed in the context of large-
18 scale variations in hydrological fluxes expected to be induced by the climate change effects. In
19 addition, Loáiciga et al. [18] pointed out that variations in groundwater extraction (anthropogenic
20 fluxes) was the predominant driver of sea water intrusion in a model that simulated sea-level rise
21 scenarios for the City of Monterrey, California. Finally, it is very likely that rising heads might
22 increase evapo-transpiration fluxes. This could impact the overall hydrological budget resulting
23 in less recharge reaching the coastal area and this will hinder the self-reversal process.

- 1 Therefore, site-specific management models for coastal areas should carefully integrate changes
- 2 in both natural and anthropogenic fluxes with various sea-level rise scenarios.

3

1 **Appendix A: Analytical comparison of salt-wedge toe positions in unconfined and confined**
2 **aquifers**

3 The basic concepts used for deriving analytical solutions for salt wedge locations using
4 the sharp-interface approximation are presented by Strack and others [23, 25-27]. Using the
5 sharp-interface approach, the toe position (X_T) in a steady-state, unconfined flow system can
6 predicted using the following expression [27]:

$$X_T = \left(\frac{q^*}{W} + L\right) - \sqrt{\left(\frac{q^*}{W} + L\right)^2 - \delta B_o^2 (1 + \delta) \left(\frac{K}{W}\right)} \quad (1A)$$

7 Where, q^* is the depth-averaged flow through the boundary per unit width of the aquifer
8 [L^2T^{-1}], B_o is the depth of aquifer bottom measured from the mean sea level [L]. W is the
9 uniform recharge rate [LT^{-1}], δ is equal to $\frac{\rho_s - \rho_f}{\rho_f}$, where ρ_f is the density of fresh water [ML^{-3}]
10 and ρ_s is the density of saltwater [ML^{-3}]. Note the above equation is purely a function of
11 groundwater flows (or fluxes) and it does not depend on boundary head levels. Hence, the
12 location of the saltwater toe position will be insensitive to changes in head levels at the sea-side
13 boundary.

14 A similar expression for estimating the toe position in a confined flow system can be
15 derived from the expressions presented by Cheng et al [23] as:

$$X_T = \left(\frac{q^*}{W} + L\right) - \sqrt{\left(\frac{q^*}{W} + L\right)^2 - \delta B^2 \left(\frac{K}{W}\right)} \quad (2A)$$

1 Where, B is the thickness of the confined aquifer [L]. Equation (2A) is similar to (1A) and the
2 only difference is the $(1 + \delta)$ term. For seawater, the value of the dimensionless parameter $\delta =$
3 0.025 , and hence the term $(1 + \delta) \sim 1$. Therefore, when $B^2K \sim B_o^2K$ (or when aquifer
4 thicknesses are matched approximately) the X_T values predicted for confined and unconfined
5 flow systems would almost be the same.

6

7

8

1 **Acknowledgments**

2 This work was, in part, supported by Auburn University graduate fellowship.

3

4 **References**

5 [1] USGS. Ground-Water Resources for the Future - Atlantic Coastal Zone. US Geological
6 Survey Fact Sheet 085-00;2000.

7

8 [2] Lacombe PJ, Carleton GB. Saltwater intrusion into fresh ground-water supplies, southern
9 Cape May County, New Jersey, 1890-1991.1992. pp. 287-98.

10

11 [3] WWD. Groundwater: the Invisible Resource. 1998.
12 <http://www.worldwaterday.org/wwday/1998/>.

13

14 [4] Li H, Jiao JJ. Tide-induced seawater-groundwater circulation in a multi-layered coastal leaky
15 aquifer system. *Journal of Hydrology* 2003;274(1-4):211-24.

16

17 [5] Michael HA, Mulligan AE, Harvey CF. Seasonal oscillations in water exchange between
18 aquifers and the coastal ocean. *Nature* 2005;436(7054):1145-8.

19

20 [6] Robinson C, Li L, Prommer H. Tide-induced recirculation across the aquifer-ocean interface.
21 *Water Resour Res* 2007;43(7):W07428. doi: 10.1029/2006wr005679

22

23 [7] Li L, Barry DA, Stagnitti F, Parlange JY. Submarine groundwater discharge and associated
24 chemical input to a coastal sea. *Water Resour Res* 1999;35(11):3253-9. doi:
25 10.1029/1999wr900189

26

27 [8] Li H, Boufadel MC, Weaver JW. Tide-induced seawater-groundwater circulation in shallow
28 beach aquifers. *Journal of Hydrology* 2008;352(1-2):211-24.

29

30 [9] Feseker T. Numerical studies on saltwater intrusion in a coastal aquifer in northwestern
31 Germany. *Hydrogeology Journal* 2007;15(2):267-79.

32

33 [10] Leatherman SP. Coastal geomorphic response to sea level rise : Galveston Bay, Texas, in
34 Barth M.C., Titus J.G. (eds) *Greenhouse effect and sea level rise : a challenge for this generation*.
35 Reinhold, New York;1984. pp. 151-78.

36

37 [11] Meisler H, Leahy PP and Knobel LL. The effect of eustatic sea-level changes on
38 saltwater-freshwater relations in the northern Atlantic Coastal Plain: U.S. Geological Survey
39 Water-Supply Paper 2255, 28 p.;1985.

- 1
2 [12] Navoy AS. Aquifer-estuary interaction and vulnerability of groundwater supplies to sea
3 level rise-driven saltwater intrusion: Pennsylvania State University, USA 1991.
4
- 5 [13] Oude Essink GHP. Salt Water Intrusion in a Three-dimensional Groundwater System in The
6 Netherlands: A Numerical Study. *Transport in Porous Media* 2001;43(1):137-58. doi:
7 10.1023/a:1010625913251
8
- 9 [14] Dausman A, Langevin C. Movement of the saltwater interface in the Surficial Aquifer
10 System in response to hydrologic stresses and water-management practices, Broward County,
11 Florida: USGS Scientific Investigations Report : SIR 2004-5256.2005.
12
- 13 [15] Melloul A, Collin M. Hydrogeological changes in coastal aquifers due to sea level rise.
14 *Ocean & Coastal Management* 2006;49(5-6):281-97.
15
- 16 [16] Ranjan P, Kazama S, Sawamoto M. Effects of climate change on coastal fresh groundwater
17 resources. *Global Environmental Change* 2006;16(4):388-99. doi:
18 10.1016/j.gloenvcha.2006.03.006
19
- 20 [17] Giambastiani BMS, Antonellini M, Oude Essink GHP, Stuurman RJ. Saltwater intrusion in
21 the unconfined coastal aquifer of Ravenna (Italy): A numerical model. *Journal of Hydrology*
22 2007;340(1-2):91-104.
23
- 24 [18] Loáiciga HA, Pingel TJ, Garcia ES. Sea Water Intrusion by Sea-Level Rise: Scenarios for
25 the 21st Century. *Ground Water* 2011:no-no. doi: 10.1111/j.1745-6584.2011.00800.x
26
- 27 [19] Werner AD, Simmons CT. Impact of Sea-Level Rise on Sea Water Intrusion in Coastal
28 Aquifers. *Ground Water* 2009.47(2):197-204. doi: 10.1111/j.1745-6584.2008.00535.x.
29
- 30 [20] Webb MD, Howard KWF. Modeling the Transient Response of Saline Intrusion to Rising
31 Sea-Levels. *Ground Water* 2010. doi: 10.1111/j.1745-6584.2010.00758.x
32
- 33 [21] IPCC. Climate change 2007: Impacts, adaptation and vulnerability. in: ML Parry, OF
34 Canziani, JP Palutikof, PJ van der Linden, CE Hanson, (Eds.). *Contribution of Working Group II*
35 *to the Fourth Assessment Report of the Intergovernmental Panel on Climate Change*. Cambridge
36 University Press Cambridge;2007.
37
- 38 [22] Vermeer M, Rahmstorf S. Global sea level linked to global temperature. *Proc Natl Acad Sci*
39 2009.106(51):21527-32. doi: 10.1073/pnas.0907765106
40
- 41 [23] Cheng AHD, Halhal D, Naji A, Ouazar D. Pumping optimization in saltwater-intruded
42 coastal aquifers. *Water Resources Research* 2000;36(8):2155-65.
43
- 44 [24] Fetter CW. *Applied Hydrogeology*. Prentice Hall, N.J., 2001.
45

- 1 [25] Strack ODL. A single-potential solution for regional interface problems in coastal aquifers.
2 Water Resources Research 1976;12(6):1165-74.
3
- 4 [26] Mantoglou A. Pumping management of coastal aquifers using analytical models of saltwater
5 intrusion. Water Resources Research 2003;39(12):1335.
6
- 7 [27] Custodio E, Bruggeman GA. Groundwater problems in coastal areas. Studies and reports in
8 hydrology 45. UNESCO, Paris;1987.
9
- 10 [28] Blanchon P, Eisenhauer A, Fietzke J, Liebetrau V. Rapid sea-level rise and reef back-
11 stepping at the close of the last interglacial highstand. Nature 2009;458(7240):881-4.
12
- 13 [29] Langevin C, Shoemaker WB, Guo W. Modflow-2000, The USGS Geological Survey
14 modular ground-water model – documentation of the Seawat-2000 version with the variable
15 density flow process (VDF) and the integrated MT3DMS transport process (IMT). US
16 Geological Survey;2003.
17
- 18 [30] Henry HR. Effects of dispersion on salt encroachment in coastal aquifers. US Geological
19 Survey Water-Supply Paper;1964. pp. C71-C84.
20
- 21 [31] Simpson MJ, Clement TP. Improving the worthiness of the Henry problem as a benchmark
22 for density-dependent groundwater flow models. Water Resour Res 2004;40(1):W01504. doi:
23 10.1029/2003wr002199
24
- 25 [32] Goswami RR, Clement TP. Laboratory-scale investigation of saltwater intrusion dynamics.
26 Water Resources Research 2007.43(4). doi: 10.1029/2006WR005151.
27
- 28 [33] Abarca E, Clement TP. A novel approach for characterizing the mixing zone of a saltwater
29 wedge. Geophys Res Lett 2009;36(6):L06402. doi: 10.1029/2008gl036995
30
- 31 [34] McCarthy JJ. Reflections On: Our Planet and Its Life, Origins, and Futures. Science
32 2009.326(5960):1646. doi: 10.1126/science.1184937.
33
- 34 [35] Anderson J, Milliken K, Wallace D, Rodriguez A, Simms A. Coastal Impact
35 Underestimated From Rapid Sea Level Rise. Eos Trans AGU 2010.91(23):205-6. doi:
36 10.1029/2010EO230001
37
- 38 [36] Abarca E, Carrera J, Sánchez-Vila X, Dentz M. Anisotropic dispersive Henry problem.
39 Advances in Water Resources 2007;30(4):913-26.
40
- 41 [37] Abarca E, Carrera J, Sánchez-Vila X, Voss CI. Quasi-horizontal circulation cells in 3D
42 seawater intrusion. Journal of Hydrology 2007;339(3-4):118-29.
43

1 **List of Figures**

2 Figure 1. Comparison of conceptual models used for visualizing the impacts of sea-level rise on
3 a saltwater wedge: (a) initial salt wedge before the sea-level rise, (b) salt wedge profile
4 after sea-level rise based on a traditional conceptual model that ignores the lifting effect,
5 and (c) a new conceptual model that includes the lifting effect.

6 Figure 2. Comparison of steady-state salt wedges predicted before and after the sea-level rise in
7 the confined system.

8 Figure 3. Transient salt wedge profiles for the confined system.

9 Figure 4. Transient variations in the toe position (X_T) and freshwater head (h_f) at the inland
10 boundary.

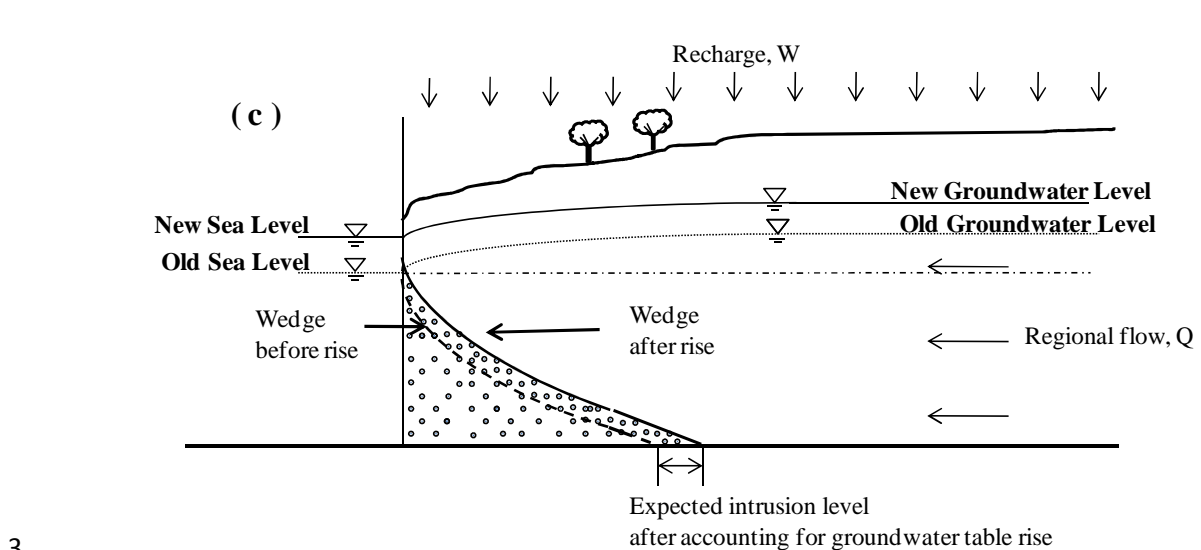
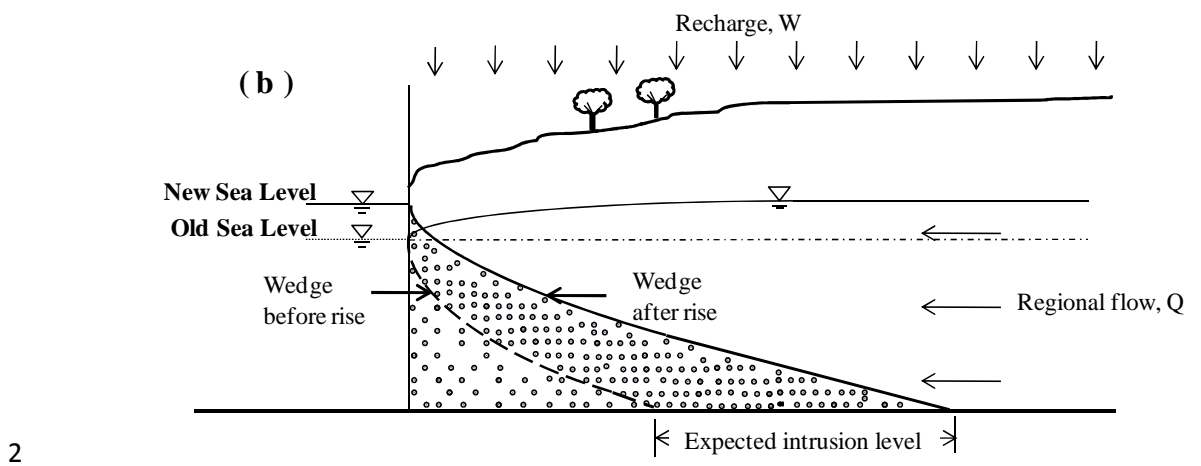
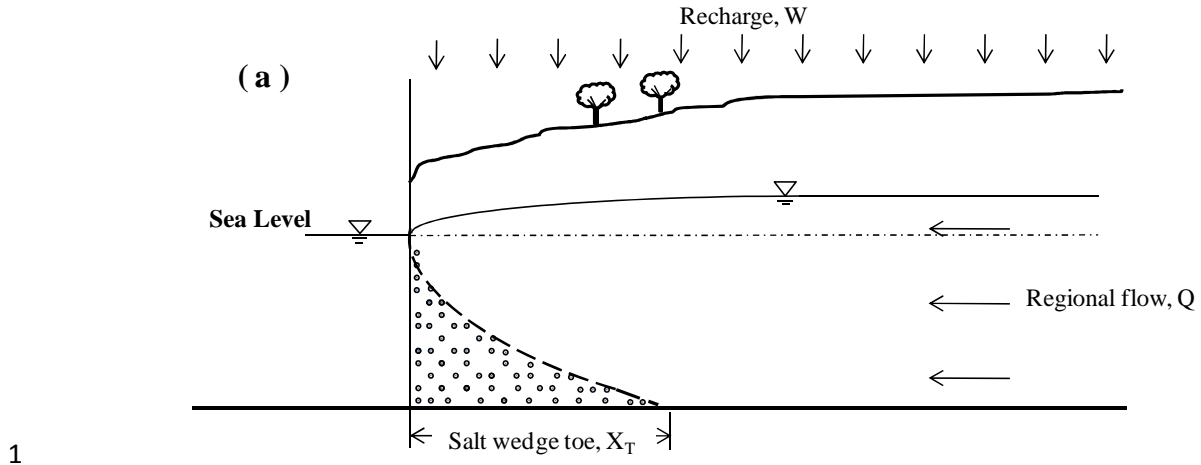
11 Figure 5. Sensitivity of the toe position (X_T) to (a) specific storage, (b) the magnitude of sea-
12 level rise, (c) the rate of sea-level rise velocity and (d) the dispersivity coefficients.

13 Figure 6. Sensitivity of the toe position (X_T) to: (a) hydraulic conductivity and (b) freshwater
14 flux.

15 Figure 7. Comparison of steady-state salt wedges predicted before the sea-level rise (sea level at
16 30m) in the unconfined- and confined-flow systems.

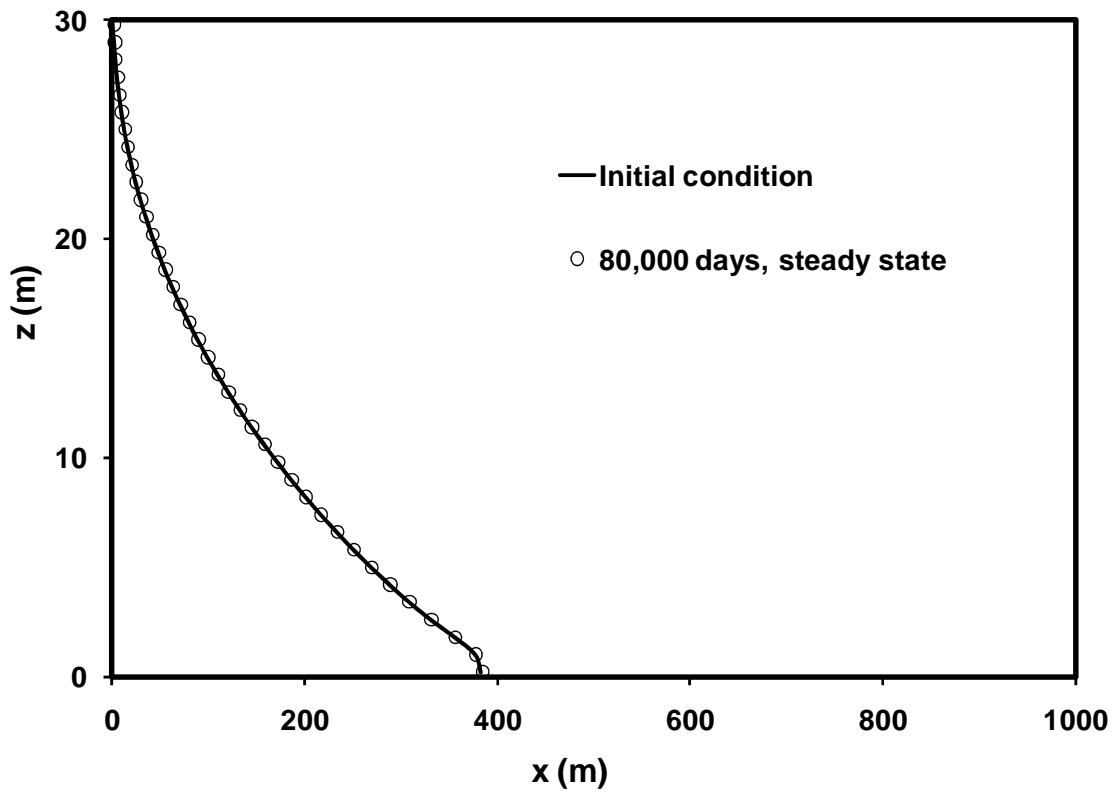
17 Figure 8. Comparison of steady-state salt wedges predicted before the sea-level rise in the
18 unconfined system, after the sea-level rise in the unconfined system, and in an
19 equivalent 34-m thick confined-flow system.

20 Figure 9. Comparison of transient variations in toe positions (X_T) predicted for the confined and
21 unconfined flow systems.



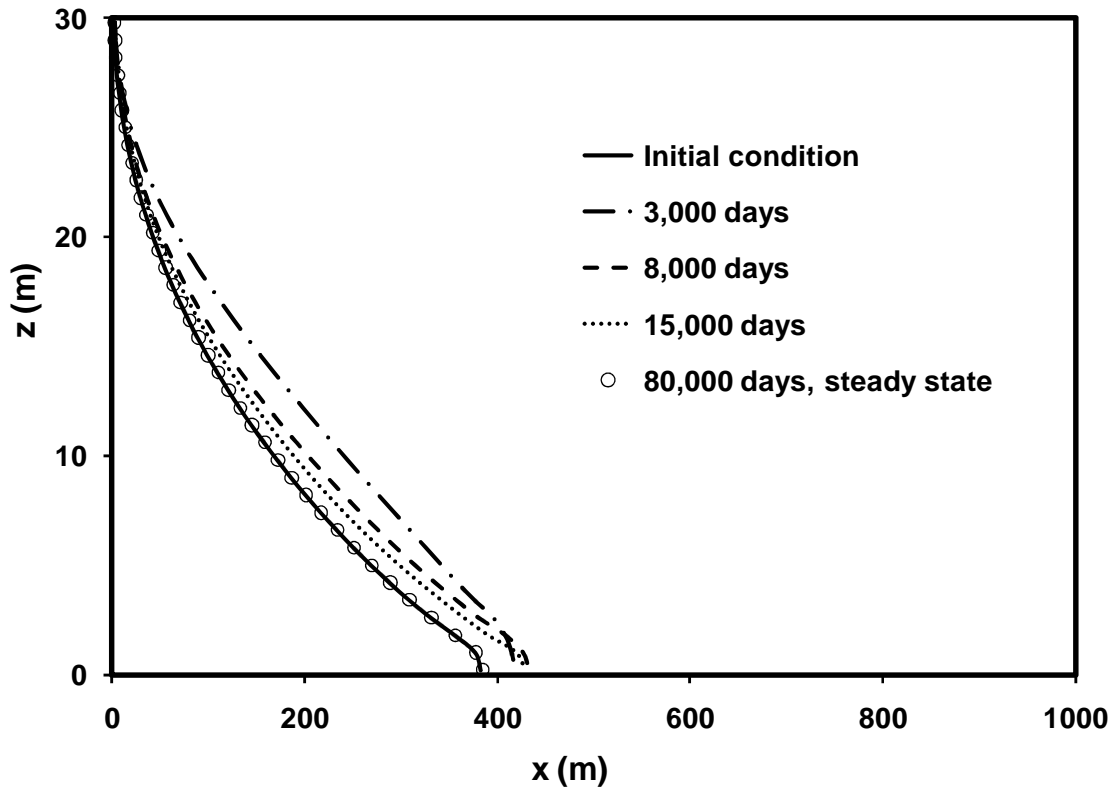
4 Figure 1. Comparison of conceptual models used for visualizing the impacts of sea-level rise on a
 5 saltwater wedge: (a) initial salt wedge before the sea-level rise, (b) salt wedge profile after sea-level rise
 6 based on a traditional conceptual model that ignores the lifting effect, and (c) a new conceptual model that
 7 includes the lifting effect.

8



1
2 Figure 2. Comparison of steady-state salt wedges predicted before and after the sea-level rise in the
3 confined system.
4

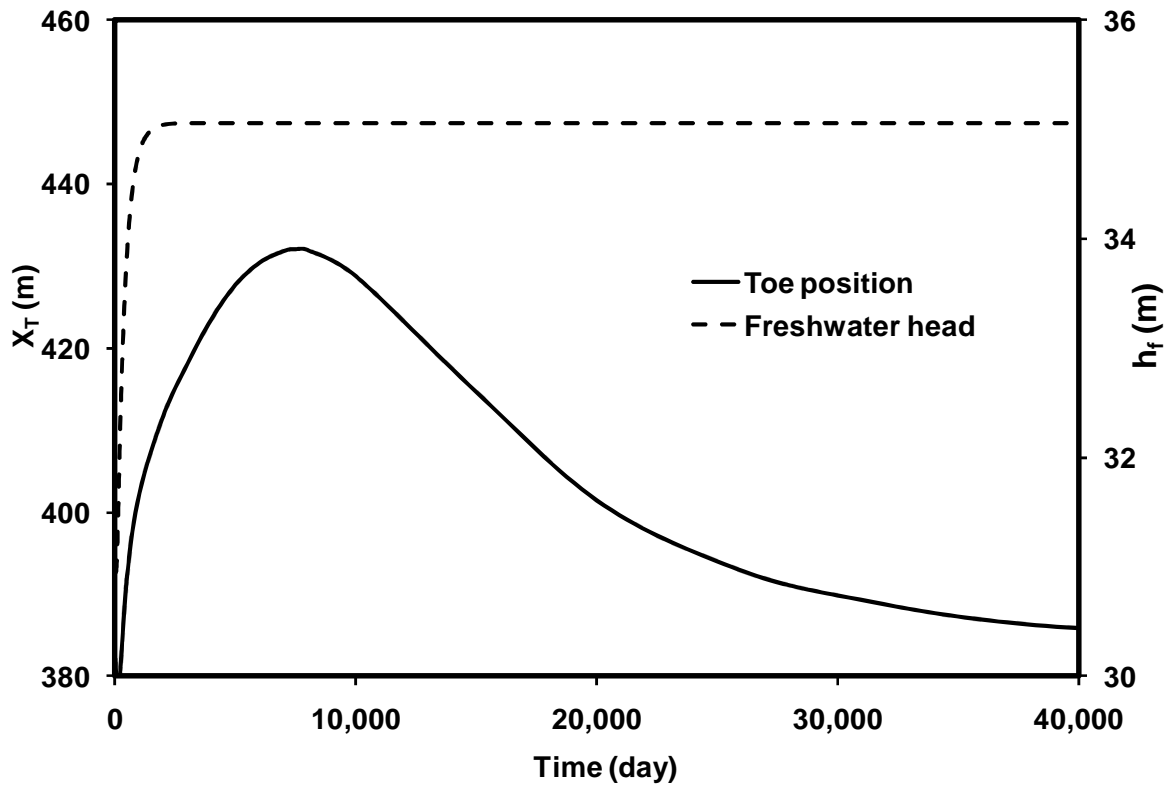
5



1

2 Figure 3. Transient salt wedge profiles for the confined system.

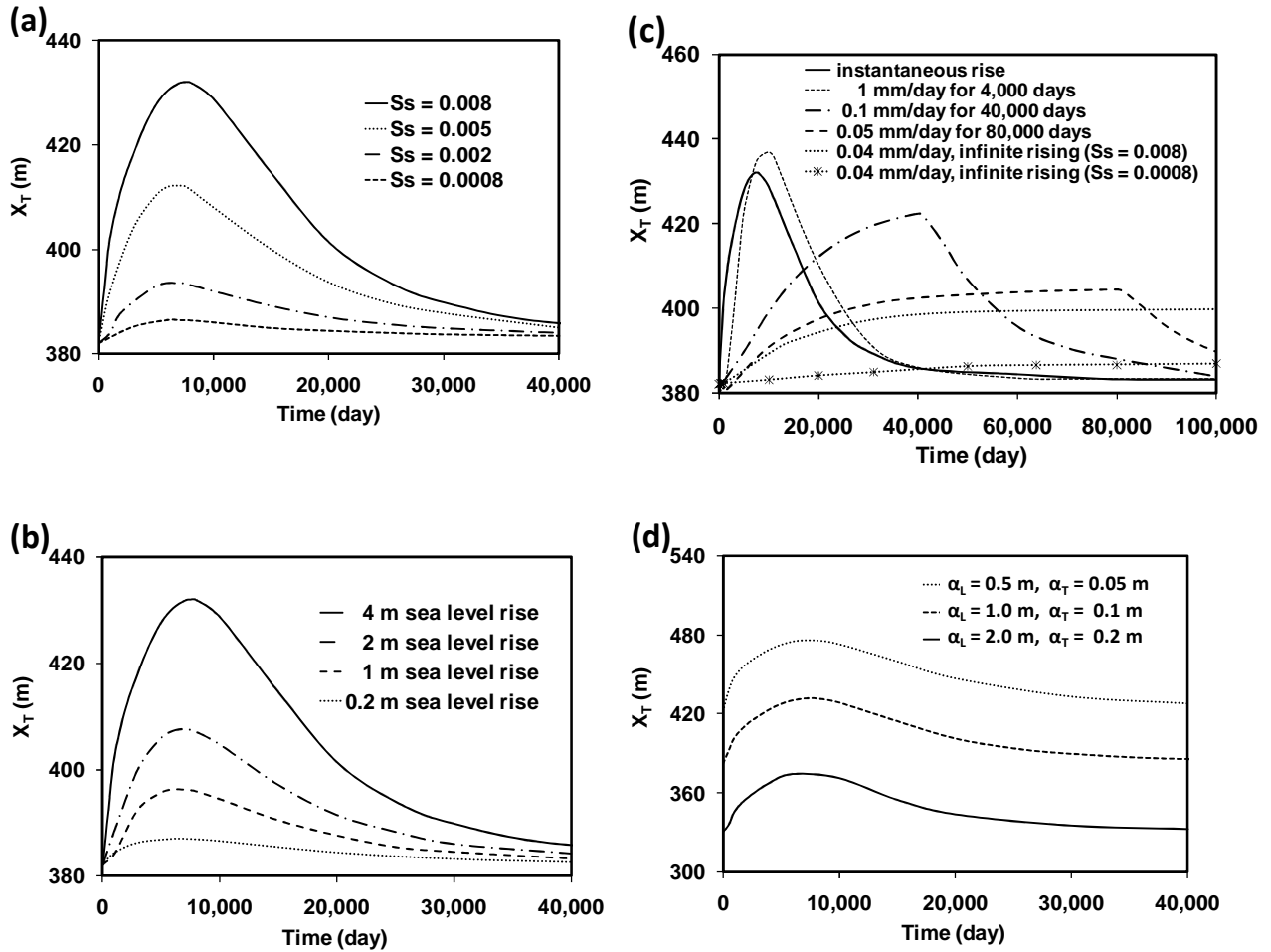
3



1

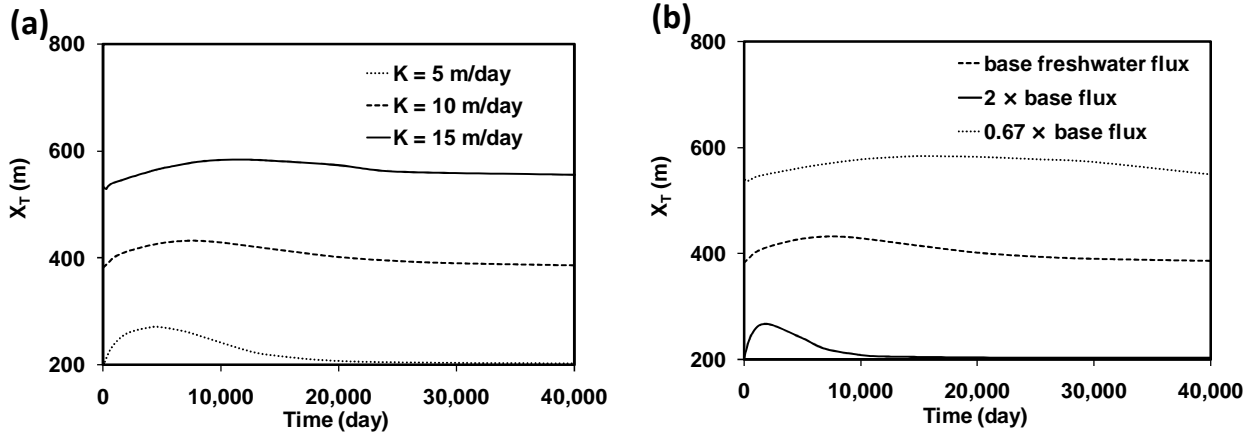
2 Figure 4. Transient variations in the toe position (X_T) and freshwater head (h_f) at the inland boundary.

3



1
2
3
4
5
6

Figure 5. Sensitivity of the toe position (X_T) to (a) specific storage, (b) the magnitude of sea-level rise, (c) the rate of sea-level rise velocity and (d) the dispersivity coefficients.

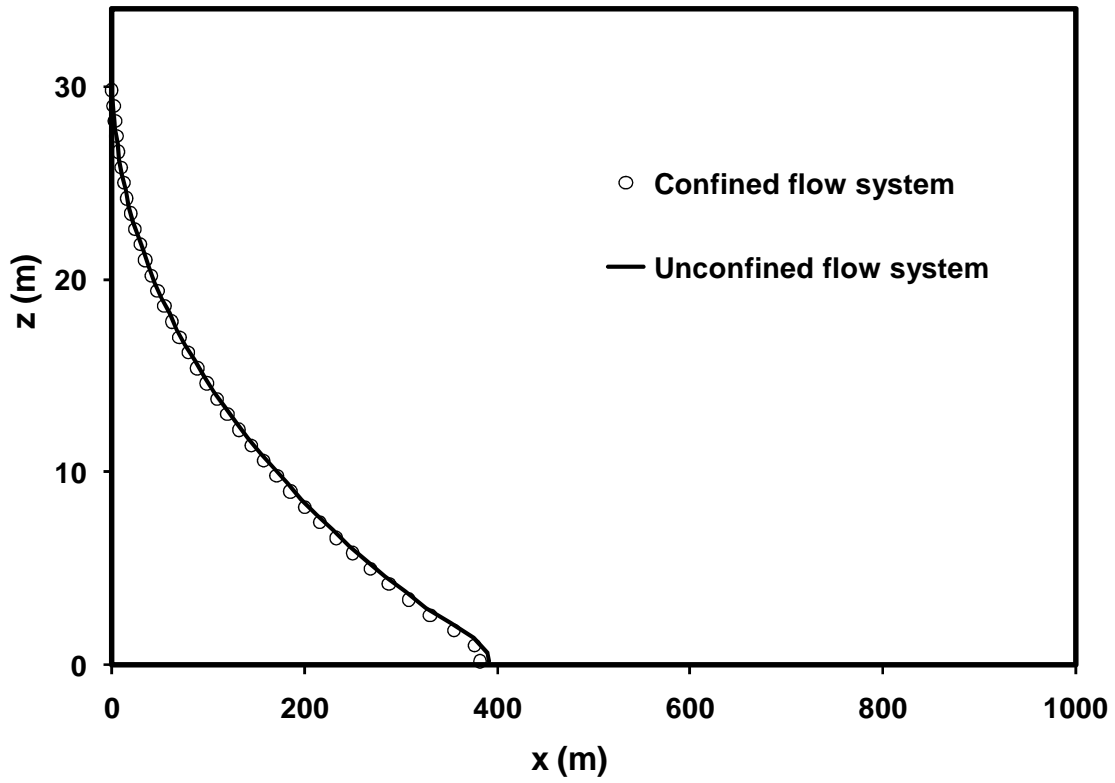


1

2

Figure 6. Sensitivity of the toe position (X_T) to: (a) hydraulic conductivity and (b) freshwater flux.

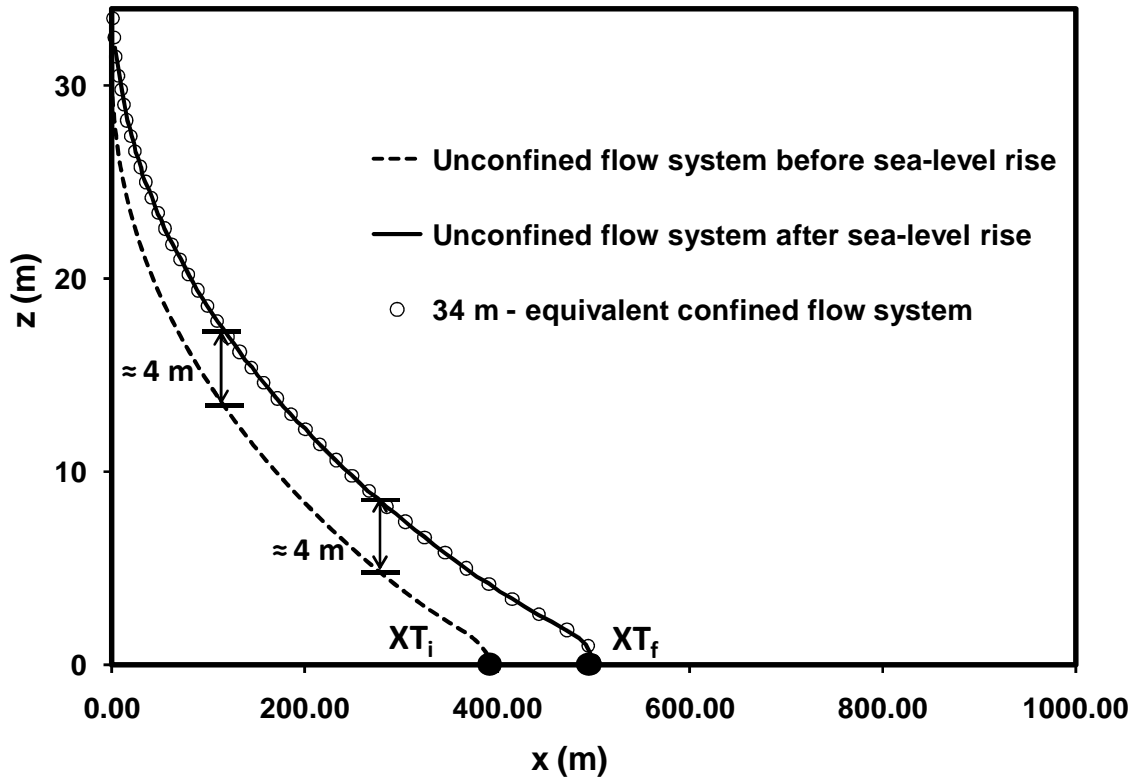
3



1

2 Figure 7. Comparison of steady-state salt wedges predicted before the sea-level rise (sea level at 30m) in
3 the unconfined- and confined-flow systems.

4



1

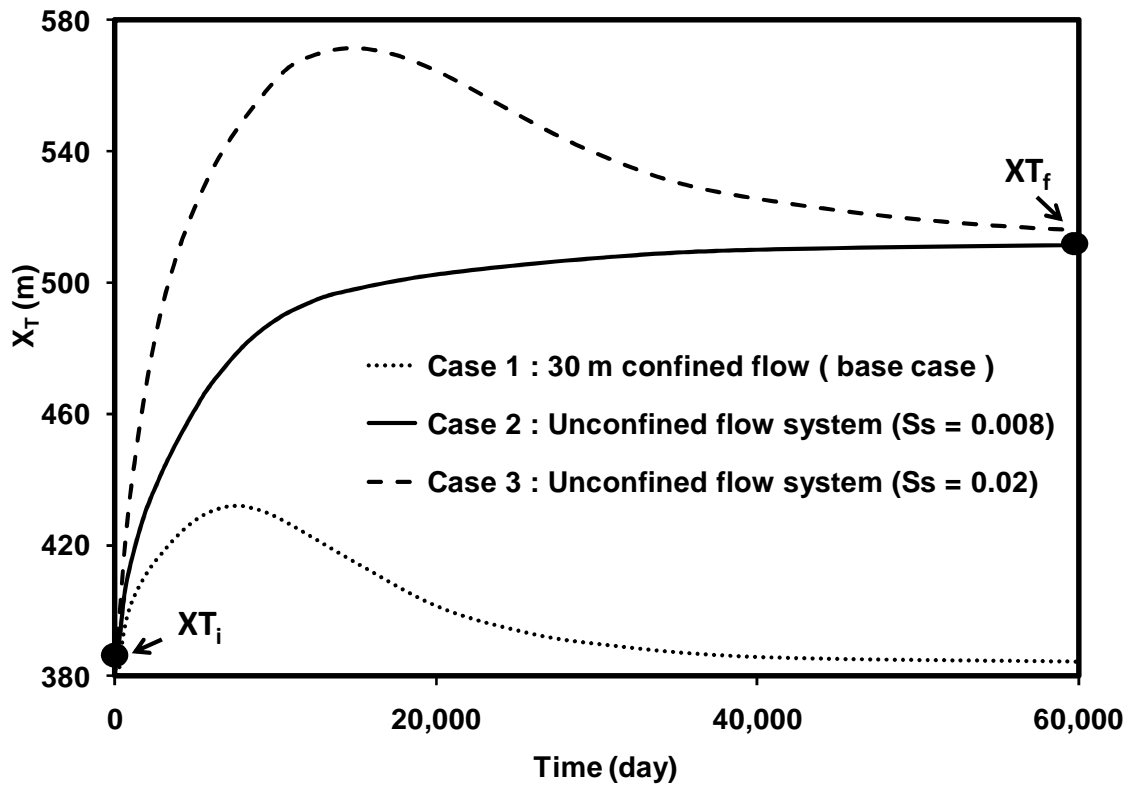
2 Figure 8. Comparison of steady-state salt wedges predicted before the sea-level rise in the unconfined
 3 system, after the sea-level rise in the unconfined system, and in an equivalent 34-m thick confined-flow
 4 system.

5

6

7

8



1

2 Figure 9. Comparison of transient variations in toe positions (X_T) predicted for the confined and
 3 unconfined flow systems.

4

1 **List of Tables**

2 Table 1. Aquifer properties and hydrological properties used for the base-case problem.

3

1 Table 1. Aquifer properties and hydrological properties used for the base-case problem.

Property	Symbol	Value
Horizontal aquifer length	L	1000 m
Vertical aquifer thickness	B	30 m
Inland groundwater flow rate	Q	0.15 m ³ /day
Uniform recharge rate from top	W	5×10 ⁻⁵ m/day
Hydraulic conductivity	K	10 m/day
Specific storage,	Ss	0.008 m ⁻¹
Longitudinal dispersivity	α _L	1 m
Transverse dispersivity	α _T	0.1 m
Saltwater concentration	C _s	35 kg/m ³
Saltwater density	ρ _s	1,025 kg/m ³
Freshwater density	ρ _f	1,000 kg/m ³

2
3
4